

## A selected ion flow tube study of the reactions of gas-phase cations with $\text{PSCl}_3$

Andrew D.J. Critchley<sup>a,1</sup>, Chris R. Howle<sup>b</sup>, Chris A. Mayhew<sup>a</sup>, Richard P. Tuckett<sup>b,\*</sup>

<sup>a</sup> School of Physics and Astronomy, University of Birmingham, Edgbaston, Birmingham B15 2TT, UK

<sup>b</sup> School of Chemistry, University of Birmingham, Edgbaston, Birmingham B15 2TT, UK

Accepted 31 March 2004

Available online 24 June 2004

### Abstract

A selected ion flow tube was used to investigate the positive ion chemistry of thiophosphoryl chloride,  $\text{PSCl}_3$ . Rate coefficients and ion product branching ratios have been determined at room temperature for reactions with 19 cations;  $\text{H}_3\text{O}^+$ ,  $\text{CF}_3^+$ ,  $\text{CF}^+$ ,  $\text{NO}^+$ ,  $\text{NO}_2^+$ ,  $\text{SF}_2^+$ ,  $\text{SF}^+$ ,  $\text{CF}_2^+$ ,  $\text{O}_2^+$ ,  $\text{H}_2\text{O}^+$ ,  $\text{N}_2\text{O}^+$ ,  $\text{O}^+$ ,  $\text{CO}_2^+$ ,  $\text{CO}^+$ ,  $\text{N}^+$ ,  $\text{N}_2^+$ ,  $\text{Ar}^+$ ,  $\text{F}^+$  and  $\text{Ne}^+$  (in order of increasing recombination energy). Complementary data described in the previous paper have been obtained for this molecule via the observation of threshold photoelectron photoion coincidences. For ions whose recombination energies are in the range 10–22 eV, comparisons are made between the product ion branching ratios of  $\text{PSCl}_3$  from photoionisation and from ion–molecule reactions. In most instances, the data from the two experiments are well correlated, suggesting that long-range charge transfer is the dominant mechanism for these ion–molecule reactions; the agreement is particularly good for the atomic ions  $\text{Ar}^+$ ,  $\text{F}^+$  and  $\text{Ne}^+$ . Some reactions (e.g.  $\text{O}_2^+ + \text{PSCl}_3$ ), however, exhibit significant differences; short-range charge transfer must then be occurring following the formation of an ion–molecule complex. For ions whose recombination energies are less than 10 eV (i.e.  $\text{H}_3\text{O}^+$ ,  $\text{CF}_3^+$ ,  $\text{CF}^+$  and  $\text{NO}^+$ ), reactions can only occur via a chemical process in which bonds are broken and formed, because the recombination energy of the cation is less than the ionisation energy of  $\text{PSCl}_3$ .

© 2004 Elsevier B.V. All rights reserved.

**Keywords:** Ion–molecule reactions; TPEPICO; Branching ratios; SIFT;  $\text{PSCl}_3$ ; Thiophosphoryl chloride

### 1. Introduction

The measurement of ion–molecule reaction rates and product distributions is of fundamental interest. These reactions are also relevant to the technological plasmas community, where a need exists for a detailed understanding of interactions occurring within plasmas which can lead to improvements in processing techniques. A better understanding of the mechanism of charge transfer, vital to plasma modelling [1], can be obtained from ion–molecule reaction studies. Chlorinated molecules are widely used in plasma etching processes, and in

this paper we present data on the reactions of a number of small gas-phase cations with thiophosphoryl chloride,  $\text{PSCl}_3$ .

Rate constants and product ion branching ratios for thermal (298 K) reactions of  $\text{PSCl}_3$  with the following cations are reported:  $\text{H}_3\text{O}^+$ ,  $\text{CF}_3^+$ ,  $\text{CF}^+$ ,  $\text{NO}^+$ ,  $\text{NO}_2^+$ ,  $\text{SF}_2^+$ ,  $\text{SF}^+$ ,  $\text{CF}_2^+$ ,  $\text{O}_2^+$ ,  $\text{H}_2\text{O}^+$ ,  $\text{N}_2\text{O}^+$ ,  $\text{O}^+$ ,  $\text{CO}_2^+$ ,  $\text{CO}^+$ ,  $\text{N}^+$ ,  $\text{N}_2^+$ ,  $\text{Ar}^+$ ,  $\text{F}^+$  and  $\text{Ne}^+$ . These ions cover a large range of recombination energies, from 6.37 eV ( $\text{H}_3\text{O}^+ + \text{e}^- \rightarrow \text{H}_2\text{O} + \text{H}$ ) to 21.56 eV ( $\text{Ne}^+ + \text{e}^- \rightarrow \text{Ne}$ ). Since the first adiabatic ionisation potential of  $\text{PSCl}_3$  has been determined from threshold photoelectron spectroscopy to be 9.70 eV (with a vertical ionisation energy of 10.41 eV) [2], both chemical reactions (i.e. the forming and breaking of bonds, important for recombination energies less than the ionisation potential) and charge transfer processes (occurring at recombination energies above the onset of ionisation) should be observed. While

\* Corresponding author. Tel.: +44-121-414-4425; fax: +44-121-414-4403.

E-mail address: [r.p.tuckett@bham.ac.uk](mailto:r.p.tuckett@bham.ac.uk) (R.P. Tuckett).

<sup>1</sup> Permanent address: AWE, Aldermaston, Reading, Berkshire RG7 4PR, UK.

charge transfer is expected to be the dominant process at higher recombination energies, chemical processes may compete if charge transfer occurs within an ion–molecule complex at short range.

We have published a review of the charge transfer (CT) process in ion–molecule reactions [3]. A long-range CT mechanism implies that the cation and neutral exert a mutual charge-induced dipole attraction, and an electron ‘jumps’ at a critical separation where the potential energy curves of  $A^+ + BC$  and  $A + BC^+$  cross. In the simple case where the potential can be expressed solely as a function of the charge-induced dipole interaction, the critical separation is inversely proportional to the difference between the recombination energy of the ion and the energy provided in ionising the neutral. This means that, for a CT process to occur at long-range (defined here as  $\geq 5 \text{ \AA}$ ), the recombination energy of the ion must be resonant with the energy required to ionise the neutral molecule BC either into the ground state or, more usually, into a vibronically excited state of  $BC^+$ . If long-range CT is unlikely, then two possibilities exist. Either the proximity of the reactants causes a perturbation in their potential energy curves which could allow a curve crossing much like the long-range mechanism, or the reactants form an ion–molecule complex in which chemical bonds are formed and broken or charge transfer occurs; that is, chemical and CT processes can compete.

In order to investigate the nature of CT processes occurring in  $PSCl_3$ , the ion–molecule reactions were compared to the fragmentation patterns of energy-selected cations produced by photoionisation of  $PSCl_3$  via the observation of threshold photoelectron–photoion coincidences (TPEPICO) [2]. The branching ratios associated with the cations formed by long-range CT should correlate closely to those of the ion fragments produced by ionisation of the neutral with a photon energy equivalent to the recombination energy of the reactant ion. Any differences in ion product branching ratios would suggest that perturbation of the initial states has occurred, resulting in changes to the branching ratios observed.

## 2. Experimental

The selected ion flow tube (SIFT) used to measure the reaction rate coefficients and product ion branching ratios has been described in detail previously [4,5]. In brief, the reagent ions were generated in an electron impact high-pressure ion source containing an appropriate gas (Ne for  $Ne^+$ ,  $CF_4$  for  $F^+$  and  $CF_x^+$  ( $x = 1-3$ ), Ar for  $Ar^+$ ,  $N_2$  for  $N^+$  and  $N_2^+$ , CO for  $CO^+$ ,  $CO_2$  for  $CO_2^+$ ,  $N_2O$  for  $O^+$ ,  $NO^+$  and  $N_2O^+$ ,  $H_2O$  for  $H_2O^+$  and  $H_3O^+$ ,  $O_2/N_2$  for  $O_2^+$ ,  $SF_6$  for  $SF_x^+$  ( $x = 1-5$ ) and  $NO_2$  for  $NO_2^+$ ). The high pressure of the gases used in the ionisation source

(several Torr) helps to quench electronically and/or vibrationally excited states of molecular ions prior to their injection into the flow tube. However, vibrational quenching is not complete, with significant vibrationally-excited populations being observed in  $O_2^+$  and  $N_2^+$  reagent ions [6]. The ion injection energy is therefore minimised, whilst maintaining a reasonable ion signal. The reagent ions were mass selected using a quadrupole mass filter, before being injected into a drift region containing high purity (99.997%) helium carrier gas typically maintained at a pressure of ca. 0.5 Torr. The buffer gas was passed through a liquid nitrogen cooled zeolite trap before use. The reagent ions were transported along the flow tube before interacting with the  $PSCl_3$  gas over a short reaction length at its far end. A capillary was used to control the amount of the reactant entering the flow tube. The loss of the reagent ions and the appearance of product ions as a function of the reactant concentration were monitored by a quadrupole mass spectrometer at the end of the flow tube. Once identified, the product ion counts were measured with degraded resolution on the detection quadrupole mass spectrometer in order to minimize mass discrimination effects. Assuming pseudo-first-order kinetics, reaction rate coefficients and ion product branching ratios were determined in the usual way [4,5,7]. Provided that no ions are being produced with the same mass as the reagent ion and that vibrationally-excited states are not present in significant numbers, the reaction rate coefficient can be extracted from a linear least-squares fit to a graph of the logarithm of the reagent ion signal versus reactant neutral concentration. Sufficient concentration of the reactant gas was used to reduce the reagent ion signal by at least 90% to ensure the graphs were linear. The rate coefficient determined represents the sum of the rates of all available channels for each reagent ion. The product ion branching ratios are only accurate to  $\pm 20\%$ , the error increasing for small branching ratios. However, since the product ion branching ratios, determined from the product ion counts as a function of reactant neutral concentration, are only used to provide a qualitative indication of the important reaction channels, no greater accuracy needs to be sought for the purposes of this investigation. Water contamination both in the flow tube and the He buffer gas resulted in electron transfer from  $H_2O$  to those injected ions whose recombination energies are greater than the ionisation potential of  $H_2O$ , 12.61 eV. This resulted in an  $H_2O^+$  signal typically  $\leq 5\%$  of the total ion signal, which is routinely corrected for in calculating product ion branching ratios. Since the reaction of  $H_2O^+$  with  $PSCl_3$  produces solely  $PSCl_2^+$ , the correction in this case was simple.

The experimental procedure for the acquisition of TPEPICO data has been described in the preceding paper [2]. Breakdown diagrams were constructed from the ion yields in the normal manner.

### 3. Results and discussion

The rate coefficients of the reactions between the 19 cations and  $\text{PSCl}_3$  are shown in Table 1, together with the product ions, the branching ratios, and the proposed neutral products. All the ions studied react with  $\text{PSCl}_3$  with a rate coefficient greater than  $10^{-10} \text{ cm}^3 \text{ s}^{-1}$  and, with the exception of  $\text{NO}^+$ , all approach the collisional limit; this latter quantity is shown in square brackets in column 2 of Table 1. These coefficients, representing unit efficiency of reaction with capture, were obtained from modified average dipole orientation calculations which utilise parameterised fits to results obtained from trajectory calculations [8]. In the absence of a literature value, the polarisability of  $\text{PSCl}_3$  was estimated to be  $1.22 \times 10^{-29} \text{ m}^3$  using the technique of Miller of adding atomic hybrid components [9], while the value used for the dipole moment of  $\text{PSCl}_3$ , 1.41 D, was that measured by Smyth et al. [10]. As found in our previous study of the ion–molecule reactions of perfluorocarbons [3], the changes in rate coefficient with recombination energy of the reactant ion did not always follow the variation of photoelectron signal with photon energy. This work suggests that long-range CT may occur provided there is an energy resonance, but its efficiency is not necessarily dependent on Franck–Condon factors.

To produce the branching ratios shown in Table 1, the experiment measured the relative intensities of ions of different masses produced from the ion–molecule reaction under consideration. The identities of the likely neutral products associated with a specific product ion were deduced via chemical reasoning. Knowledge of the constituent atoms of the reactant ion and the co-reactant was sufficient in most cases to make an unambiguous determination of the ionic products. However, some ambiguities still remain, particularly in the reactions of  $\text{CF}_x^+$  with  $\text{PSCl}_3$  since  $\text{P}^+$  has the same mass as  $\text{CF}^+$ , but thermochemical arguments helped to restrict the number of possible channels. The channels considered most plausible for each reaction are listed in Table 1. The majority of the enthalpies of formation at 298 K used for the thermochemical calculations were taken from standard sources [11,12]. The values used for the enthalpies of formation of  $\text{CF}_x$ ,  $\text{CF}_x^+$  and  $\text{SF}_x$ ,  $\text{SF}_x^+$  were taken from Ricca [13] and Bauschlicher and Ricca [14], respectively, from coupled cluster ab initio calculations. The enthalpies of formation of  $\text{PSCl}_2^+$  and  $\text{PCl}_2^+$  were determined from the appearance energy at 298 K ( $AE_{298}$ ) for these ions from  $\text{PSCl}_3$  and  $\text{PCl}_3$  in complementary TPEPICO experiments [2,15], allowance being made for the small correction needed to convert  $AE_{298}$  of a fragment ion into  $\Delta_f H_{298}^0$  for the unimolecular reaction [16]. Upper limit enthalpies of formation of 629 ( $\text{PSCl}_2^+$ ) and 722 ( $\text{PCl}_2^+$ )  $\text{kJ mol}^{-1}$  were obtained [2]. Values for  $\Delta_f H_{298}^0$  of  $\text{PCl}^+$  and  $\text{PSCl}^+$  are unknown, and shown as such in column 5 of Table 1. Many of the  $\Delta_f H_{298}^0$  values

for the proposed neutral products are also unknown, and shown accordingly.

#### 3.1. Reactions of ions with recombination energies below the onset of ionisation of $\text{PSCl}_3$

At low recombination energy, ions are produced that are formed from bond cleavage and formation in ion–molecule complexes. The reaction between  $\text{H}_3\text{O}^+$  and  $\text{PSCl}_3$  proceeds exclusively via proton transfer to  $\text{HPSCl}_3^+$ , indicating that the proton affinity of  $\text{PSCl}_3$  is greater than that of water.  $\text{O}^+$  transfer occurs with  $\text{NO}_2^+$ ,  $\text{OPSCl}_3^+$  being the major product. The reactions of  $\text{NO}^+$  and  $\text{CF}^+$  with  $\text{PSCl}_3$  warrant some discussion. A significant amount of  $\text{NO} \cdot \text{PSCl}_3^+$  is formed from the first reaction, but the major product is  $\text{PSCl}_3^+$  (47%). As the rate constant observed is less than a quarter of the capture value, one might expect this reaction to be slightly endothermic, and indeed the energy available from the recombination of  $\text{NO}^+$  is significantly less than the experimentally-determined ionisation energy of  $\text{PSCl}_3$ . It has been found, however, that a significant amount of vibrationally excited  $\text{NO}^+$  is created in selected ion flow tubes by electron impact ionisation [17], which may account for the shortfall in the energy available to the reaction; the  $v = 2$  level of  $\text{NO}^+ \text{X}^1\Sigma^+$  has a recombination energy of 9.83 eV, making its reaction with  $\text{PSCl}_3$  just exothermic. Despite this fact, the majority of the ions should be in the ground vibrational state, making it difficult to account for a 47% branching ratio for this channel. Furthermore, 7% of the products of this reaction are  $\text{PSCl}_2^+$  ions, which is even more endothermic than production of  $\text{PSCl}_3^+$ . We note that the endothermicities for production of  $\text{PSCl}_2^+ + \text{ClNO}$  given in Table 1 are upper limits, and they will take lower values if  $\Delta_f H_{298}^0(\text{PSCl}_2^+)$  is significantly less than 629  $\text{kJ mol}^{-1}$ . A possible mechanism for the formation of  $\text{PSCl}_3^+$  and  $\text{PSCl}_2^+$  is via collisionally-induced dissociation of  $\text{NO} \cdot \text{PSCl}_3^+$  as it accelerates into the detection region.

Unlike  $\text{NO}^+$ , the major difficulty in interpreting the  $\text{CF}^+$  data is that of product assignment. The major product of the reaction of  $\text{CF}^+$  with  $\text{PSCl}_3$ , with a yield of 64%, has mass 63 u. Its identity could be  $\text{CFS}^+$  or  $\text{PS}^+$ . The production of  $\text{CFS}^+$  requires the breaking of one P=S bond, whilst that of  $\text{PS}^+$  needs three P–Cl bonds to break. The reaction  $\text{CF}^+ + \text{PSCl}_3 \rightarrow \text{CFS}^+ + \text{PCl}_3$  is exothermic, provided  $\Delta_f H_{298}^0(\text{CFS}^+)$  is less than 1037  $\text{kJ mol}^{-1}$ . However, the  $\text{PS}^+$  channel is also exothermic, since the reaction  $\text{CF}^+ + \text{PSCl}_3 \rightarrow \text{PS}^+ + \text{CFCl}_3$  has an enthalpy of reaction,  $\Delta_f H_{298}^0 = -13 \text{ kJ mol}^{-1}$ . Evidence from other reactions illustrates that the three P–Cl bonds may be broken. Thus,  $\text{N}^+$  unambiguously produces  $\text{PS}^+$ , admittedly at a low level of 1%, via the same chemical mechanism ( $\text{N}^+ + \text{PSCl}_3 \rightarrow \text{PS}^+ + \text{NCl}_3$ ;  $\Delta_f H_{298}^0 = -203 \text{ kJ mol}^{-1}$ ). However, the reaction also produces  $\text{NS}^+$  at the 5% level via the same potential mechanism for pro-

Table 1

Rate coefficients at 298 K, product cations, branching ratios, and suggested neutral products for the reactions of 19 cations with PSCl<sub>3</sub>

Reagent ion (RE/eV)	Rate coefficient/10 <sup>-9</sup> cm <sup>3</sup> s <sup>-1</sup>	Product ions (%)	Proposed neutral products	$\Delta_r H_{298}^0$ /kJ mol <sup>-1</sup>
H <sub>3</sub> O <sup>+</sup> (6.37)	1.9 [2.6]	H · PSCl <sub>3</sub> <sup>+</sup> (100)	H <sub>2</sub> O	-443 + $\Delta_r H^0$ (H · PSCl <sub>3</sub> <sup>+</sup> )
CF <sub>3</sub> <sup>+</sup> (9.04)	1.1 [1.6]	PSCl <sub>2</sub> <sup>+</sup> (48) CF <sub>3</sub> · PSCl <sub>3</sub> <sup>+</sup> (44) PFCl <sub>3</sub> <sup>+</sup> (8)	CClF <sub>3</sub> - CF <sub>2</sub> S	-106 -27 + $\Delta_r H^0$ (CF <sub>3</sub> · PSCl <sub>3</sub> <sup>+</sup> ) -377 + $\Delta_r H^0$ (PFCl <sub>3</sub> <sup>+</sup> )
CF <sup>+</sup> (9.12)	1.9 [2.1]	<i>PS</i> <sup>+</sup> and/or <i>CFS</i> <sup>+</sup> (64) PFCl <sub>2</sub> <sup>+</sup> (15) <i>PCl</i> <sub>2</sub> <sup>+</sup> and/or <i>CFCI</i> <sub>2</sub> <sup>+</sup> (9) CFSCl <sub>3</sub> <sup>+</sup> (7) PFCl <sub>3</sub> <sup>+</sup> (4) CClS <sup>+</sup> (1)	CCl <sub>3</sub> F PCl <sub>3</sub> CClS CClFS PSCl P CS PFCl <sub>2</sub>	-13 -1037 + $\Delta_r H^0$ (CFS <sup>+</sup> ) -748 + $\Delta_r H^0$ (PFCl <sub>2</sub> <sup>+</sup> ) + $\Delta_r H^0$ (CClS) -26 + $\Delta_r H^0$ (CClFS) -45 + $\Delta_r H^0$ (PSCl) -432 + $\Delta_r H^0$ (CFSCl <sub>3</sub> <sup>+</sup> ) -468 + $\Delta_r H^0$ (PFCl <sub>3</sub> <sup>+</sup> ) +187 + $\Delta_r H^0$ (CClS <sup>+</sup> ) + $\Delta_r H^0$ (PFCl <sub>2</sub> )
NO <sup>+</sup> (9.26)	0.49 [2.2]	PSCl <sub>3</sub> <sup>+</sup> (47) NO · PSCl <sub>3</sub> <sup>+</sup> (33) PCl <sub>2</sub> <sup>+</sup> (13) PSCl <sub>2</sub> <sup>+</sup> (7)	NO - CINOS CINO	+42, +15, -13 <sup>a</sup> -604 + $\Delta_r H^0$ (NO · PSCl <sub>3</sub> <sup>+</sup> ) +365 + $\Delta_r H^0$ (CINOS) +77, +50, +22 <sup>a</sup>
NO <sub>2</sub> <sup>+</sup> (9.75)	1.8 [1.8]	O · PSCl <sub>3</sub> <sup>+</sup> (97) NO · PSCl <sub>3</sub> <sup>+</sup> (3)	NO O	-504 + $\Delta_r H^0$ (O · PSCl <sub>3</sub> <sup>+</sup> ) -345 + $\Delta_r H^0$ (NO · PSCl <sub>3</sub> <sup>+</sup> )
SF <sub>2</sub> <sup>+</sup> (10.15)	1.4 [1.5]	PSCl <sub>3</sub> <sup>+</sup> (66) S · PSCl <sub>3</sub> <sup>+</sup> (13) FS <sub>2</sub> <sup>+</sup> (8) PFCl <sub>3</sub> <sup>+</sup> (8) PCl <sub>3</sub> <sup>+</sup> (5)	SF <sub>2</sub> F <sub>2</sub> PFCl <sub>3</sub> FS <sub>2</sub> SSF <sub>2</sub>	-43 -304 + $\Delta_r H^0$ (S · PSCl <sub>3</sub> <sup>+</sup> ) +507 + $\Delta_r H^0$ (PFCl <sub>3</sub> <sup>+</sup> ) -304 + $\Delta_r H^0$ (PFCl <sub>3</sub> <sup>+</sup> ) + $\Delta_r H^0$ (FS <sub>2</sub> ) -38
SF <sup>+</sup> (10.22)	1.6 [1.7]	PSCl <sub>3</sub> <sup>+</sup> (69) PSCl <sub>2</sub> <sup>+</sup> (14) PFCl <sub>3</sub> <sup>+</sup> (6) ClS <sub>2</sub> <sup>+</sup> (4) PCl <sub>3</sub> <sup>+</sup> (3) S <sub>2</sub> <sup>+</sup> (2) S · PSCl <sub>3</sub> <sup>+</sup> (2)	SF SFCl S <sub>2</sub> ClF + ClP FS <sub>2</sub> PFCl <sub>3</sub> F	-50 +20 + $\Delta_r H^0$ (SFCl) -1110 + $\Delta_r H^0$ (PFCl <sub>3</sub> <sup>+</sup> ) -530 + $\Delta_r H^0$ (ClS <sub>2</sub> <sup>+</sup> ) +58 + $\Delta_r H^0$ (FS <sub>2</sub> ) +422 + $\Delta_r H^0$ (PFCl <sub>3</sub> <sup>+</sup> ) -530 + $\Delta_r H^0$ (S · PSCl <sub>3</sub> <sup>+</sup> )
CF <sub>2</sub> <sup>+</sup> (11.45)	1.4 [1.7]	PSCl <sub>3</sub> <sup>+</sup> (69) PCl <sub>3</sub> <sup>+</sup> (25) PSCl <sub>2</sub> <sup>+</sup> (4) <i>PFCl</i> <sub>3</sub> <sup>+</sup> and/or <i>CF<sub>2</sub>Cl</i> <sub>3</sub> <sup>+</sup> (2)	CF <sub>2</sub> CF <sub>2</sub> S CClF <sub>2</sub> CFS PS	-169 -215 -178 -532 + $\Delta_r H^0$ (PFCl <sub>3</sub> <sup>+</sup> ) + $\Delta_r H^0$ (CFS) -393 + $\Delta_r H^0$ (CF <sub>2</sub> Cl <sub>3</sub> <sup>+</sup> )
O <sub>2</sub> <sup>+</sup> (12.07)	1.6 [2.1]	PSCl <sub>3</sub> <sup>+</sup> (73) PSCl <sub>2</sub> <sup>+</sup> (21) O <sub>2</sub> · PSCl <sub>2</sub> <sup>+</sup> (6)	O <sub>2</sub> Cl + O <sub>2</sub> Cl	-229 -35 -664 + $\Delta_r H^0$ (O <sub>2</sub> · PSCl <sub>2</sub> <sup>+</sup> )
H <sub>2</sub> O <sup>+</sup> (12.61)	2.0 [2.7]	PSCl <sub>2</sub> <sup>+</sup> (100)	Cl + H <sub>2</sub> O	-87
N <sub>2</sub> O <sup>+</sup> (12.89)	1.6 [1.8]	PSCl <sub>2</sub> <sup>+</sup> (93) PCl <sub>2</sub> <sup>+</sup> (6) PSCl <sub>3</sub> <sup>+</sup> (1)	Cl + N <sub>2</sub> O SCl + N <sub>2</sub> O N <sub>2</sub> O	-114 +14.6 -308
O <sup>+</sup> (13.62)	2.4 [2.8]	PSCl <sub>2</sub> <sup>+</sup> (69) PSCl <sub>3</sub> <sup>+</sup> (18) PCl <sub>2</sub> <sup>+</sup> (13)	Cl + O O SCl + O	-184 -378 -55
CO <sub>2</sub> <sup>+</sup> (13.77)	1.7 [1.8]	PSCl <sub>2</sub> <sup>+</sup> (80) PSCl <sub>3</sub> <sup>+</sup> (11) PCl <sub>2</sub> <sup>+</sup> (6) O <sub>2</sub> · PSCl <sub>2</sub> <sup>+</sup> (3)	Cl + CO <sub>2</sub> CO <sub>2</sub> SCl + CO <sub>2</sub> CCl	-198 -392 -70 -53 + $\Delta_r H^0$ (O <sub>2</sub> · PSCl <sub>2</sub> <sup>+</sup> )
CO <sup>+</sup> (14.01)	1.9 [2.2]	PSCl <sub>2</sub> <sup>+</sup> (93) PCl <sub>2</sub> <sup>+</sup> (6) PSCl <sub>3</sub> <sup>+</sup> (1)	Cl + CO SCl + CO CO	-221 -93 -415

Table 1 (continued)

Reagent ion (RE/eV)	Rate coefficient/ $10^{-9}$ $\text{cm}^3 \text{s}^{-1}$	Product ions (%)	Proposed neutral products	$\Delta_r H_{298}^0/\text{kJ mol}^{-1}$
$\text{N}^+$ (14.53)	2.4 [3.0]	$\text{PSCI}_2^+$ (62)	Cl + N	-272
		$\text{PSCI}_3^+$ (16)	N	-466
		$\text{PCI}_2^+$ (15)	SCI + N	-144
		$\text{NS}^+$ (5)	$\text{PCI}_3$	-665
		$\text{PSCI}^+$ (1)	$\text{Cl}_2 + \text{N}$	$-1022 + \Delta_r H^0(\text{PSCI}^+)$
		$\text{PS}^+$ (1)	$\text{NCl}_3$	-203
$\text{N}_2^+$ (15.58)	2.0 [2.2]	$\text{PSCI}_2^+$ (80)	Cl + $\text{N}_2$	-373
		$\text{PCI}_2^+$ (14)	SCI + $\text{N}_2$	-245
		$\text{PSCI}^+$ (4)	$\text{Cl}_2 + \text{N}_2$	$-1123 + \Delta_r H^0(\text{PSCI}^+)$
		$\text{PSCI}_3^+$ (2)	$\text{N}_2$	-567
$\text{Ar}^+$ (15.76)	1.7 [1.9]	$\text{PSCI}^+$ (39)	$\text{Cl}_2 + \text{Ar}$	$-1140 + \Delta_r H^0(\text{PSCI}^+)$
		$\text{PSCI}_2^+$ (38)	Cl + Ar	-391
		$\text{PCI}_2^+$ (21)	SCI + Ar	-263
		$\text{PSCI}_3^+$ (2)	Ar	-585
$\text{F}^+$ (17.42)	2.0 [2.6]	$\text{PS}^+$ (38)	$\text{Cl}_2 + \text{ClF}$	-406
		$\text{PCI}_2^+$ (22)	SCI + F	-422
		$\text{PSCI}^+$ (17)	$\text{Cl}_2 + \text{F}$	$-1300 + \Delta_r H^0(\text{PSCI}^+)$
		$\text{PSCI}_2^+$ (15)	Cl + F	-550
		$\text{PCI}^+$ (5)	$\text{SCL}_2 + \text{F}$	$-1318 + \Delta_r H^0(\text{PCI}^+)$
		$\text{PSCI}_3^+$ (3)	F	-745
$\text{Ne}^+$ (21.56)	2.0 [2.6]	$\text{PS}^+$ (46)	$\text{Cl}_2 + \text{Cl} + \text{Ne}$	-555
		$\text{PCI}^+$ (36)	$\text{SCL}_2 + \text{Ne}$	$-1718 + \Delta_r H^0(\text{PCI}^+)$
		$\text{PCI}_2^+$ (7)	SCI + Ne	-822
		$\text{PSCI}_2^+$ (5)	Cl + Ne	-950
		$\text{PSCI}_3^+$ (3)	Ne	-1144
		$\text{PSCI}^+$ (2)	$\text{Cl}_2 + \text{Ne}$	$-1700 + \Delta_r H^0(\text{PSCI}^+)$
		$\text{S}^+$ (1)	$\text{PCI}_3 + \text{Ne}$	-707
		Cl <sup>+</sup> (trace)	$\text{P} + \text{SCL}_2 + \text{Ne}$	-30

The recombination energy of the ion is shown in column 1. Experimental rate coefficients are shown in column 2; values in square brackets are theoretical capture coefficients (see text). The product ions and their branching ratios are shown in column 3; ambiguities in the products are shown in italics. The most likely accompanying neutral products are given in column 4, with the enthalpy of the proposed reaction given in column 5.

<sup>a</sup> The three values quoted are for the enthalpy of reaction at 298 K involving the  $v = 0, 1,$  and  $2$  levels of the ground electronic state of  $\text{NO}^+$ .

ducing  $\text{CFS}^+$  ( $\text{N}^+ + \text{PSCI}_3 \rightarrow \text{NS}^+ + \text{PCI}_3$ ;  $\Delta_r H_{298}^0 = -665 \text{ kJ mol}^{-1}$ ). We conclude that the product ion of mass 63 u in the  $\text{CF}^+ + \text{PSCI}_3$  reaction is an unknown combination of  $\text{CFS}^+$  and  $\text{PS}^+$ . Examination at higher resolution was unable to determine the specific composition of the combined peak, as both products have one sulphur atom and hence an isotope of similar intensity at mass 65 u. The parent ion signal was not sufficient to permit the observation of  $^{13}\text{C}^{19}\text{F}^{34}\text{S}$  with mass 66 u. This ambiguity is also present in the reactions of  $\text{CF}_2^+$  and  $\text{CF}_3^+$ , however most of the alternative products are unlikely to occur due to the extensive rearrangement required within the reaction complex. Where a significant ambiguity exists, both possible channels are presented in italics in column 3 of Table 1.

### 3.2. Reactions of ions with recombination energies above the onset of ionisation of $\text{PSCI}_3$

The adiabatic ionisation potential of  $\text{PSCI}_3$  is 9.70 eV and the threshold for production of  $\text{PSCI}_2^+$  is 11.55 eV

[2]. For ions whose recombination energy spans 10.15–11.55 eV (i.e.  $\text{SF}_2^+$ ,  $\text{SF}^+$  and  $\text{CF}_2^+$ ) the major product ion is  $\text{PSCI}_3^+$ , presumably formed via long-range CT. For ions with recombination energy greater than 11.55 eV, reactions proceed via dissociative CT. As observed in the reactions of saturated and unsaturated perfluorocarbons [3], the degree of fragmentation increases with increasing recombination energy. We note, however, that there is still some branching ratio from non-dissociative CT producing  $\text{PSCI}_3^+$  even at the highest recombination energy studied, 21.56 eV.

Fig. 1 of the preceding paper [2] shows the threshold photoelectron spectrum of  $\text{PSCI}_3$  and the coincident ion yields following dissociative photoionisation at a resolution of 0.3 nm. Four product ions are observed;  $\text{PSCI}_3^+$ ,  $\text{PSCI}_2^+$ ,  $\text{PXCl}^+$  and  $\text{PX}^+$ , where  $\text{X} = \text{S}$  or  $\text{Cl}$ . The difficulties of resolving the masses of  $\text{PSCI}^+$  from  $\text{PCI}_2^+$  and  $\text{PS}^+$  from  $\text{PCI}^+$  were discussed earlier [2]. The parent ion is dominant up to 11.5 eV,  $\text{PSCI}_2^+$  becomes dominant for  $h\nu > 11.8$  eV,  $\text{PCI}_2^+$  shows a low yield of ca. 10% for  $h\nu > 12$  eV and  $\text{PSCI}^+$  shows a greater yield

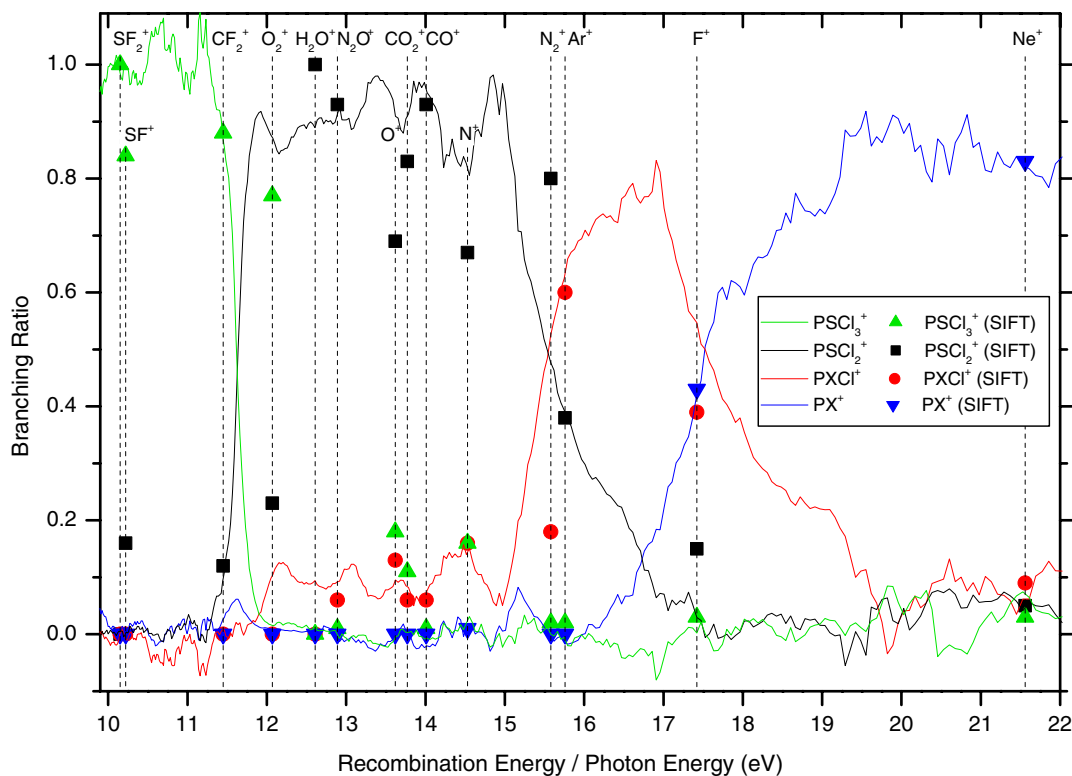


Fig. 1. Comparison of the products from ion–molecule studies of  $\text{PSCl}_3$  with TPEPICO photoionisation branching ratios over the energy range 10–22 eV. A colour version of this figure is available electronically on the web.

for  $h\nu > 15.2$  eV, and  $\text{PX}^+$  shows a very weak yield for  $h\nu > 16$  eV. The solid lines of Fig. 1 of this paper show the resulting breakdown diagram over this photon range of 10–22 eV. For simplicity, we have shown only the yields of unresolved  $\text{PXCl}^+$  and  $\text{PX}^+$ . The individual data points shown in Fig. 1 give the branching ratios from the ion–molecule reactions for the product ions that could result from CT over this same range of ion recombination energies, 10–22 eV. We consider the results in two groups; ions with recombination energy in the range 10–15 eV, and those in the range 15–22 eV.

For ions with recombination energies between 10 and 15 eV ( $\text{SF}_2^+$  through  $\text{N}^+$ ), the major product ions are  $\text{PSCl}_3^+$ ,  $\text{PSCl}_2^+$  and  $\text{PCl}_2^+$ . These ions are also observed in the photon-induced study [2]. With the exception of the  $\text{O}_2^+$  data, there is reasonable agreement between the product ion branching ratios from the photon- and ion-induced reactions. This suggests that long-range CT, both non-dissociative and dissociative, is the dominant mechanism for ion–molecule reactions of  $\text{PSCl}_3$  with ions whose recombination energy lies in the range 10–15 eV. We note that the yield of  $\text{PSCl}_2^+$  reaches 100% for the reaction of  $\text{H}_2\text{O}^+$  with  $\text{PSCl}_3$ , and suggests that a large Franck–Condon overlap exists between neutral  $\text{PSCl}_3$  and an excited vibronic state of  $\text{PSCl}_3^+$  that dissociates to  $\text{PSCl}_2^+ + \text{Cl}$  at the recombination energy of  $\text{H}_2\text{O}^+$ , 12.61 eV. This is confirmed by the threshold photoelectron spectrum (Fig. 1(a) of [2]).

We now consider the anomalous data for  $\text{O}_2^+$  (12.07 eV) and, to a lesser extent, aspects of the  $\text{H}_2\text{O}^+$  data. The  $\text{O}_2^+ + \text{PSCl}_3$  reaction produces  $\text{PSCl}_3^+$  as the dominant ion, whilst photoexcitation of  $\text{PSCl}_3$  at 12.07 eV produces  $\text{PSCl}_2^+$  as the dominant ion. This phenomenon can probably be explained by the presence of  $\text{O}_2 \cdot \text{PSCl}_3^+$  at the 6% level. An ion–molecule complex must form to produce this product, and it is therefore not surprising that the  $\text{PSCl}_2^+$  relative yields from the two experiments do not match. At a lower level of disagreement, the reactions of  $\text{O}_2^+$  and  $\text{H}_2\text{O}^+$  with  $\text{PSCl}_3$  produce zero yield of  $\text{PCl}_2^+$ , whereas photoexcitation in the range 12.1–12.6 eV produces this ion with a yield of ca. 10%. Using the value for  $\Delta_f H_{298}^0(\text{PCl}_2^+)$  of  $722 \text{ kJ mol}^{-1}$  derived from dissociative photoionisation of  $\text{PCl}_3$  [15], the reaction  $\text{PSCl}_3 + h\nu \rightarrow \text{PCl}_2^+ + \text{SCl} + e^-$  requires the photon energy to be at least 12.88, 15.35 eV if the neutral products are  $\text{S} + \text{Cl}$ .  $\text{PCl}_2^+$ , however, has an  $AE_{298}$  of 11.8 eV from  $\text{PSCl}_3$  [2]. The disparity in these results was noted in the previous paper, and cannot be explained. We note that  $\text{PCl}_2^+$  is not observed as a CT product from any ion–molecule reaction unless the recombination energy of the ion is greater than that of  $\text{N}_2\text{O}^+$ , 12.89 eV. This observation is therefore consistent with the thermochemistry for  $\text{PCl}_2^+$  derived from the  $\text{PCl}_3 + h\nu \rightarrow \text{PCl}_2^+ + \text{Cl} + e^-$  reaction [15].

We now consider ions with recombination energy in the range 15–22 eV. For the three atomic ions in this

range,  $\text{Ar}^+$ ,  $\text{F}^+$  and  $\text{Ne}^+$ , the trend of increasing fragmentation with increasing recombination energy is apparent. Thus with  $\text{Ar}^+$ ,  $\text{PSCl}_2^+$  and  $\text{PSCl}^+$  are the dominant ions with approximately equal branching ratios. With  $\text{F}^+$ ,  $\text{PCl}_2^+$  and  $\text{PS}^+$  are the two most dominant ions. With  $\text{Ne}^+$ ,  $\text{PS}^+$  and  $\text{PCl}^+$  are the two dominant ions. Furthermore, the branching ratios mimic very closely those from the photon-induced study (Fig. 1). This is particularly strong evidence to support the theory that, for the reactions of these three atomic ions, long-range CT dominates. The results for the reaction of  $\text{N}_2^+$  (15.58 eV) with a similar recombination energy to that of  $\text{Ar}^+$ , however, are slightly anomalous. This is the photon energy where the relative yield of  $\text{PSCl}_2^+$  is reducing steeply as that of  $\text{PSCl}^+$  increases steeply. At 15.58 eV, the branching ratio for production of  $\text{PSCl}_2^+$  from photoionisation is ca. 0.5, whereas the yield of this ion from  $\text{N}_2^+ + \text{PSCl}_3$  is 0.80. Likewise, the combined yield of  $\text{PSCl}^+$  and  $\text{PCl}_2^+$  from the photon experiment is also ca. 0.5 whereas the yield of these two ions from the ion–molecule reaction is only 0.18. This would suggest that the potential curves of the reactants are being perturbed in the ion–molecule reaction, and charge transfer is occurring at a shorter distance [3].

Finally, we note that in the range 10–22 eV  $\text{PCl}_3^+$  was not observed as a product of dissociative photoionisation or as a product of any CT ion–molecule reaction. In addition, a study of the fragment ions produced from 70 eV electron impact ionisation of  $\text{PSCl}_3$  found that the yield of  $\text{PCl}_3^+$  was also very low [18]. This suggests that there is no energy resonance between  $\text{PSCl}_3$  and a potential curve that dissociates to  $\text{PCl}_3^+ + \text{S}$ . While the  $\text{P}=\text{S}$  bond is never broken exclusively in long-range dissociative CT,  $\text{PCl}_3^+$  is observed when a short-range interaction takes place. Thus for the  $\text{CF}_2^+$  reaction,  $\text{S}^-$  abstraction via the reaction  $\text{CF}_2^+ + \text{PSCl}_3 \rightarrow \text{PCl}_3^+ + \text{CF}_2\text{S}$  is the only exothermic pathway that can produce  $\text{PCl}_3^+$ , and this channel has a significant branching ratio of 25%.  $\text{S}^-$  abstraction was also observed in the reactions of the  $\text{SF}_x^+$  ions.

#### 4. Conclusions

The reactions of 19 ions with  $\text{PSCl}_3$  have been studied, with data presented for the rate constants and the product ion branching ratios. With the exception of  $\text{NO}^+ + \text{PSCl}_3$ , all reactions proceed at or close to the collisional limit. For those ions with recombination energies greater than the ionisation energy of  $\text{PSCl}_3$ , 9.70 eV, dissociative charge transfer is the dominant process. Thus in the energy range of 10–22 eV, the charge transfer products observed via ion–molecule reactions

are in most instances in good agreement with photoionisation fragment distributions obtained from threshold photoelectron photoion coincidence data. The agreement is particularly good for the three high-energy atomic ions,  $\text{Ar}^+$ ,  $\text{F}^+$  and  $\text{Ne}^+$ . However, for some reactions marked differences have been observed,  $\text{O}_2^+ + \text{PSCl}_3$  being the most notable example. In these instances, the results indicate that short-range charge transfer must be occurring within an ion–molecule complex. For those ions with recombination energies less than 9.70 eV, a chemical reaction occurring within the ion–molecule complex is the only mechanisms available to produce the observed products.

#### Acknowledgements

We thank the Technological Plasma Initiative Programme of EPSRC (GR/L82083) for financial support of this study, and Clair Atterbury and Ray Chim for help in recording the data. Andrew Critchley and Chris Howle thank EPSRC for a research fellowship and a research studentship, respectively.

#### References

- [1] A. Bogaerts, R. Gijbels, *J. Anal. Atom. Spectrom.* 11 (1996) 841.
- [2] C.R. Howle, R.Y.L. Chim, R.P. Tuckett, A.E.R. Malins, *Chem. Phys.* 303 (2004) 227.
- [3] G.K. Jarvis, R.A. Kennedy, C.A. Mayhew, R.P. Tuckett, *Int. J. Mass Spectrom.* 202 (2000) 323.
- [4] D. Smith, N.G. Adams, *Adv. Atom. Mol. Phys.* 24 (1988) 1.
- [5] N.G. Adams, D. Smith, in: J.M. Farrar, W.H. Saunders (Eds.), *Techniques for the Study of Ion–Molecule Reactions*, Wiley, New York, 1988, p. 165.
- [6] G.K. Jarvis, C.A. Mayhew, R.P. Tuckett, *J. Phys. Chem.* 100 (1996) 17166.
- [7] D. Smith, N.G. Adams, *Int. J. Mass Spectrom. Ion Phys.* 21 (1976) 349.
- [8] T. Su, W.J. Chesnavich, *J. Chem. Phys.* 76 (1982) 5183.
- [9] K.J. Miller, *J. Am. Chem. Soc.* 112 (1990) 8533.
- [10] C.P. Smyth, G.L. Lewis, A.J. Grossman, F.B. Jennings III, *J. Am. Chem. Soc.* 62 (1940) 1219.
- [11] M.W. Chase Jr., *NIST-JANAF Thermochemical Tables*, *J. Phys. Chem. Ref. Data*, Monograph, 4th ed. 9 (2000).
- [12] S.J. Lias, J.E. Bartmess, J.F. Liebman, J.L. Holmes, R.D. Levin, W.G. Mallard, *J. Phys. Chem. Ref. Data Suppl.* 1 (1988) 17.
- [13] A. Ricca, *J. Phys. Chem. A* 103 (1999) 1876.
- [14] C.W. Bauschlicher, A. Ricca, *J. Phys. Chem. A* 102 (1998) 4722.
- [15] K.J. Boyle, G.K. Jarvis, R.P. Tuckett, *J. Chem. Soc., Faraday Trans.* 94 (1998) 1045.
- [16] J.C. Traeger, R.G. McLoughlin, *J. Am. Chem. Soc.* 103 (1981) 3647.
- [17] D.A. Fairley, D.B. Milligan, C.G. Freeman, M.J. McEwan, P. Spanel, D. Smith, *Int. J. Mass Spectrom.* 193 (1999) 35.
- [18] R.J. Matthews, *Int. J. Mass Spectrom. Ion Phys.* 14 (1974) 75.